Journal of Solid State Chemistry **162,** 327–332 (2001)
doi:10.1006/jssc.2001.9329, available online at http://www.idealibrary.com on IDEAL®

Two Ternary Phases Containing Sb_2^{4-} Ions: $Na_2M_3Sb_4$, M= Sr, Ba. Synthesis, Structure, and Properties

Lisheng Chi and John D. Corbett[1]

Ames Laboratory–DOE[2] and Department of Chemistry, Iowa State University, Ames, Iowa 50011

Received March 29, 2001; in revised form June 12, 2001; accepted July 30, 2001

IN HONOR OF PROFESSOR PAUL HAGENMULLER ON THE OCCASSION OF HIS 80TH BIRTHDAY

The isotypic compounds $Na_2Ba_3Sb_4$ and $Na_2Sr_3Sb_4$ were prepared by the direct fusion of elements at 750°C followed by slow cooling to, and annealing at, 300°C. These crystallize in the orthorhombic system, space group *Pnma* (No. 62), with respective lattice dimensions of a = 8.220(1), 7.919(2) Å; b = 17.136(3), 16.526(5) Å; c = 9.140(2), 8.801(2) Å; V = 1287.5(2), 1151.7(4) Å^3; and Z = 4. The structure of $Na_2Ba_3Sb_4$ was refined from single-crystal X-ray data. All antimony atoms are dimerized as two independent Sb_2^{4-} units which, together with a Na atom, center quadrilateral prisms of Ba or Sr and Na. The structure can be directly related to that of β-Ba_5Sb_4 (Eu_5As_4, *Cmca*) by an oxidative distortion on cation substitution that allows the dimerization of the isolated Sb^{3-} anions therein. The barium compound is a Zintl phase, being established as diamagnetic and semiconducting ($\rho_{294} \simeq 570$ μΩ cm).

1. INTRODUCTION

Many compounds of the type A_5B_4 between active metals A (groups 1–4) and post-transition elements B afford a fascinating series of phases that demonstrate the general strong tendency of the B elements to polymerize so as to yield or approach valence-precise Zintl phases (1). This tendency may of course be attenuated by electronic factors or by the advantages of electron delocalization with a parallel increase in Madelung energy when extra cations are incorporated (2). One prominent parent structure type, orthorhombic (*Pnma*) Sm_5Ge_4 (3), exhibits an equal number of dimer (formally Ge_2^{6-}) and monomer (Ge^{4-}) anions, but there is also a distorted version in the same space group for Gd_5Si_4 (4), Tb_5Si_4, and Dy_5Si_4 (5) that contains only silicon dimers. Three extra delocalized electrons remain in the latter, so that these compounds are presumably also metallic and do not meet formal Zintl–Klemm concepts. (Many other R_5Tt_4-type phases for the rare-earth elements (R) with Tt = Si–Pb have been assigned the Sm_5Ge_4 structure (6), largely on the basis of Debye–Scherrer powder patterns from which such a distinction is probably not possible.) Recent intense interest has developed regarding mixed dimorphic $Gd_5(Si_xGe_{1-x})_4$ examples because a phase transition to monoclinic symmetry occurs with breaking of half of the Tt–Tt bonds (7–9) and gives rise to a variety of diverse, unique, and large magnetoresponsive phenomena (10–12). It also appears probable that one can control the equilibrium dimer–monomer distribution in R_5Tt_4 phases by varying the free electron concentration, as has been shown by the attainment of the Gd_5Si_4 (all dimer) type for La_5Ge_3Ga (13) and by the present work.

When the valence states in Gd_5Si_4, etc. are altered by replacement of the trivalent cations by lower field Eu^{2+} ions and substitution of the tetrel atom Si by the pnictogen As, the space group increases in symmetry from *Pnma* to *Cmca*, and the anions nominally become two isolated As^{3-} and one dumbbell As_2^{4-} anions (14). As a result, the compound Eu_5As_4 is structurally a Zintl phase and is presumably a diamagnetic semiconductor (assuming Eu^{2+}), although this does not seem to have been verified. Both Sm_5Ge_4 and Eu_5As_4 structure types are known for Ba_5Sb_4 (15,16), the latter, higher symmetry Zintl phase (assigned as β) reasonably coming from synthesis at lower temperature. (The former was misidentified as Gd_5Si_4 type.) The von Schnering group (17,18) later obtained compounds of the type $Na_2M_3Pn_4$ (M = Eu, Sr; Pn = P, As), ternary variants of the Eu_5As_4-type structure (*Pnma*), through substitution of 40% of the dipositive cations by monovalent sodium. In this case, the two formerly isolated anions become oxidized and all of the pnictogen atoms appear as dimers, As_2^{4-} or P_2^{4-}. This structure was shown to be a ternary distortion variant

[1]To whom correspondence should be addressed. Fax: 515-294-5718. E-mail: jcorbett@iastate.edu.

[2]This research was supported by the Office of the Basic Energy Sciences, Materials Sciences Division, U.S. Department of Energy. The Ames Laboratory is operated by DOE by Iowa State University under Contract No. W-7405-Eng-82. Accordingly, the U.S. Government retains a nonexclusive, royalty-free license to publish or reproduce the published form of the contribution, or to allow others to do so for U.S. Government purposes.

0022-4596/01 $35.00

of the *Cmca* structure of Eu_5As_4. No properties relevant to the presumed Zintl constitution of these two compounds or of β-Ba_5Sb_4 have appeared. In the present work, we sought to dimerize all of the antimony ions in β-Ba_5Sb_4 $[(Ba^{2+})_5(Sb^{3-})_2Sb_2^{4-}]$ (*Cmca*) by replacement of two Ba^{2+} ions with two Na^+ ions. This led to the parallel discovery of two new ternary antimonides, $Na_2Ba_3Sb_4$ and $Na_2Sr_3Sb_4$, in the same space group *Pnma*. We report here their syntheses, structure, and some properties.

2. EXPERIMENTAL

2.1. Synthesis

The general techniques of synthesis in welded Ta tubing containers, glovebox use, and Guinier powder diffraction have been described before (19–21). All the reagents and products were handled in N_2- or He-filled gloveboxes with moisture levels less than 0.1 ppm vol. The reagents employed, all from Alfa-Aesar, were Na (3–9's), K (99.95%), Sr (3–9's), Ba (3–9's) (both distilled), and Sb (6–9's). The alkaline-earth metals were usually first heated in sealed Ta tubes under high vacuum at 100–200°C below their melting points for 8–24 h to remove any pervasive hydrogen impurities (22, 23), whereas the surfaces of all of the metals as received were first cut clean with a scalpel. (The first step also allowed us to establish that α-Ba_5Sb_4 does not contain hydride as a necessary component.) Reactions were run on a $\sim$200-mg scale in welded 9-mm-o.d. Ta tubing. The first compound $Na_2Ba_3Sb_4$ was initially obtained from the loaded composition Na:Ba:Sb = 2:1:2, which was inserted in a cleaned tantalum tube already welded at one end, the other end was tightly crimped in the glovebox, and the tube was welded shut under argon. The tantalum container in turn was protected from the atmosphere within a fused silica ampoule sealed under high vacuum. The system was heated at 750°C for 12 h, slowly cooled to 280°C at 2°C/h, and equilibrated there for 72 h. The quenched product was a black matrix that contained a large number of well-shaped crystals. Their stoichiometry $Na_2Ba_3Sb_4$ was first determined by single-crystal X-ray diffraction analysis. The pure phase was subsequently obtained (according to its Guinier powder pattern) from a sample with the indicated composition after this had been heated to 750°C for 12 h, cooled to 300°C at 2°C/h, and equilibrated at this temperature for 7 days. The $Na_2Sr_3Sb_4$ analogue was synthesized similarly. The equivalent bismuth phases could not be synthesized.

2.2. Structure Determination

A few well-shaped black, reflective crystals from the first reaction were picked up in a N_2-filled crystal box with a little grease, sealed in thin-walled capillaries, and checked by Laue and Weissenberg photographs for their singularity and quality. One with approximate dimensions of $0.1 \times 0.15 \times 0.2$ mm was chosen for data collection, which was carried out at room temperature on a Rigaku AFC6R single-crystal diffractometer with the aid of graphite-monochromated Mo$K\alpha$ radiation. Programmed indexing of 21 reflections from a random search over $22.3^\circ < 2\theta < 33.8^\circ$ yielded an orthorhombic cell of dimensions $a = 8.192(2)$ Å, $b = 17.093(3)$ Å, $c = 9.106(2)$ Å, $V = 1275.1(4)$ Å^3. A Laue check revealed an *mmm* class. Two octants of data were collected using an Ω–2θ scan to $2\theta_{max}$ of 60° with a scan speed of 16°/min and a scan width of $(0.94 + 0.34 \tan\theta)$ deg. A total of 3644 reflections was measured, of which 1885 were independent and observed ($I > 2\sigma(I_o)$) and used for structure solution and refinement.

The TEXSAN program package (24) was used for data processing. The raw data were corrected for Lorentz and polarization effects, and for absorption empirically with the aid of ψ-scans of three reflections ($\mu = 174.6$ cm^{-1}). The systematic absence conditions, $0kl$: $k + l = 2n$; $hk0$: $h = 2n$, suggested space group $Pn2_1a$ or *Pnma*, and the intensity statistics ($|E^2 - 1| = 0.953$) led to the latter centric space group for the structure solution.

The structure was solved by direct methods and refined by the full-matrix least-squares on F^2. The first step yielded five positions, of which two were assigned to Ba atoms and

TABLE 1
Crystal and Structure Refinement Data for $Na_2Ba_3Sb_4$

Formula weight	945.00
Temperature, K	293(2)
Crystal system	Orthorhombic
Space group, Z	*Pnma*, 4
Unit cell dimensions (Å, Å^3)[a]	
a	8.220(1)
b	17.136(3)
c	9.140(2)
V	1287.5(2)
Density (calculated), g/cm^3	4.923
Absorption coefficient (Mo $K\alpha$, mm^{-1})	17.462
$F(000)$	1576
Crystal size, mm	$0.1 \times 0.15 \times 0.2$
Theta range for data collection, deg	2.38 to 30.00°
Completeness to $\theta = 30.00°$	98.4%
Index ranges	$-11 \le h \le 11$, $0 \le k \le 24$, $-11 \le l \le 0$
Reflections collected	3644
Independent reflections	1885 [R(int) = 0.102]
Refinement method	Full-matrix least-squares on F^2
Data/restraints/parameters	1150/0/48
Goodness-of-fit	0.974
Final R indices [$I > 2\sigma(I)$][b]	$R1 = 0.041$, w$R2 = 0.084$
(all data)	$R1 = 0.103$, w$R2 = 0.100$
Sec. extinct. coeff.	0.0035(2)
Largest diff. peak and hole, e$^-$ Å^{-3}	2.45 and −1.75

[a] Refined from Guinier data with Si as internal standard, $\lambda = 1.540562$ Å, 23°C.

[b] $R1 = \sum||F_o| - |F_c||/\sum|F_o|$; w$R2 = [\sum w(|F_o|^2 - |F_c|^2)^2/\sum w(F_o^2)^2]^{1/2}$.

TABLE 2
Atomic Coordinates ($\times 10^4$) and Displacement Parameters ($Å^2 \times 10^3$) for $Na_2Ba_3Sb_4$

Atom	x	y	z	U (eq)[a]
Na[b]	1496(11)	2500	4852(10)	44(2)
Ba	4896(1)	4033(1)	3122(1)	16(1)
M[c]	3287(2)	3708(1)	8212(1)	18(1)
Sb1[b]	221(1)	2500	9167(1)	18(1)
Sb2[b]	2752(1)	2500	1326(1)	15(1)
Sb3	1554(1)	4637(1)	5335(1)	17(1)

Atom	U_{11}[d]	U_{22}	U_{33}	U_{12}	U_{13}	U_{23}
Na	26(4)	68(6)	39(5)	0	4(4)	0
Ba	13(1)	22(1)	14(1)	3(1)	1(1)	2(1)
M	17(1)	20(1)	15(1)	2(1)	0(1)	1(1)
Sb1	15(1)	23(1)	17(1)	0	2(1)	0
Sb2	12(1)	17(1)	16(1)	0	2(1)	0
Sb3	15(1)	22(1)	13(1)	4(1)	1(1)	(1)

[a] U(eq) is defined as one third of the trace of the orthogonalized U_{ij} tensor.
[b] On mirror plane at $y = \frac{1}{4}$
[c] $M = 0.5$ Na + 0.5 Ba.
[d] The anisotropic displacement factors take the form: $-2\pi^2[h^2a^{*2}U_{11} + \ldots. + 2hka^*b^*U_{12}..]$.

three to Sb atoms according to the distribution and distances around each position. A single independent residual (~ 18 e/ Å^3) in a higher symmetry position in the subsequent difference Fourier synthesis was assigned to the Na atom. However, the Ba2 position assigned earlier exhibited an abnormally large displacement parameter when first refined, which implied a statistical disorder of the cations (or a deficiency of barium) in this position. This was reassigned as a statistical mixture of Ba and Na atoms, for which the site occupancy factors of Ba2 and Na2 converged at 0.487(6) and 0.513(6), respectively, when constrained to a sum of unity. Because these values were within $\sim 2\sigma$ of 0.5, the value expected for charge balance in a valence compound, this proportion was used in later refinements without any significant changes appearing. (The later direct synthesis of the pure compound for the indicated composition $Na_2Ba_3Sb_4$ validated this treatment.)

TABLE 3
Bond lengths (Å) for $Na_2Ba_3Sb_4$

Sb1–Sb2	2.867(2)	Na–M	3.791(8) × 2
Sb3–Sb3	2.907(2)	Na–M	3.985(8) × 2
Sb1–Na	3.191(9)	Ba–Sb1	3.621(1)
Sb1–M[a]	3.376(2) × 2	Ba–Sb2	3.560(1)
Sb1–M	3.397(2) × 2	Ba–Sb2	3.564(1)
Sb1–Ba	3.621(1) × 2	Ba–Sb3	3.593(1)
Sb2–Sb1	2.867(2)	Ba–Sb3	3.620(1)
Sb2–Na	3.260(9)	Ba–Sb3	3.962(1)
Sb2–Na	3.384(9)	Ba–Na	4.002(7)
Sb2–M	3.547(2) × 2	Ba–Na	4.149(7)
Sb2–Ba	3.560(1) × 2	Ba–Ba	4.2644(9) × 2
Sb2–Ba	3.564(1) × 2	Ba–M	4.325(2)
Sb3–Na	3.689(2)	M–Sb1	3.376(2)
Sb3–M	3.388(2)	M–Sb1	3.397(2)
Sb3–M	3.393(2)	M–Sb2	3.549(2)
Sb3–M	3.439(2)	M–Sb3	3.388(2)
Sb3–Ba	3.593(1)	M–Sb3	3.393(2)
Sb3–Ba	3.620(1)	M–Sb3	3.439(2)
Sb3–Ba	3.962(1)	M–Na	3.791(8)
Na-Sb2	3.260(9)	M–Na	3.985(8)
Na–Sb2	3.384(9)	M–M	4.140(3)
Na–Sb3	3.689(2)	M–M	4.3112(1) × 2

[a] $M = 0.5$Ba + 0.5Na.

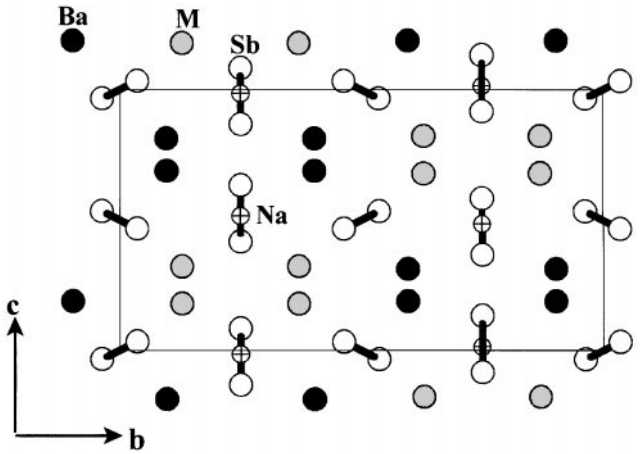

FIG. 1. [100] projection of the orthorhombic structure of $Na_2Ba_3Sb_4$ (*Pnma*): Ba, black, M (0.5 Na, 0.5 Ba), gray, Sb, white, Na, small crossed white circles. The bonds in Sb_2 units are represented by wider black lines.

After isotropic refinement of all positions, the $R1$ value was 5.9%, and the six highest electron density peaks in a difference map, ≤ 6.8 e$^-$/ Å^3, were all within 0.55 Å of Ba or Sb. The final anisotropic refinement of $I > 2\sigma_I(I)$ data converged at $R1 = 4.13\%$ and $wR2 = 8.45\%$ for 48 variables. The maximum and minimum peaks in the final difference Fourier map were 2.49 e/ Å^3 and -1.75 e/ Å^3. All calculations were performed with the SHELXTL program package (25). The distances reported for $Na_2Ba_3Sb_4$ were calculated with the aid of the more accurate lattice dimensions refined from its Guinier powder pattern with Si (NIST) as an internal standard ($\lambda = 1.540562$ Å). These values differed from those obtained on the diffractometer by 0.03 to 0.04 Å (11–14σ). Some details of the crystallography and refinement parameters in the study of $Na_2Ba_3Sb_4$ are listed in Table 1. The structure factor data are available from J.D.C.

2.3. *Physical Properties*

Electrical resistivities of a single-phase sample of $Na_2Ba_3Sb_4$ were measured at 34 MHz by the electrodeless

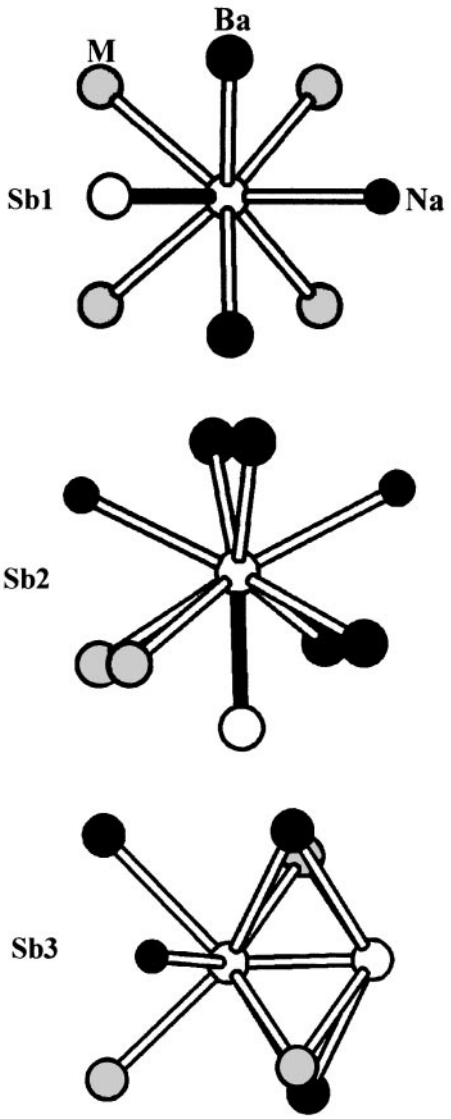

FIG. 2. The environments of the three types of antimony atoms in Sb1–Sb2 dimers and Sb3–Sb3 dimers, respectively. Nearest neighbors are trigonal prismatic Ba and M, augmented by face-capping Na or Sb, as labelled.

"Q" method over a range of 110–294 K (26). The powdered 81.1 mg sample that had been sieved to a grain size between 150 and 250 μm was dispersed in chromatographic Al_2O_3. Magnetic susceptibilities of the same sample were obtained at a field of 3 T over a range of 6–300 K with the aid of a Quantum Design (MPMS) SQUID magnetometer. A sample of 22.0 mg was held between two fused silica rods within a tightly fitting outer silica tube and sealed under He. The susceptibilities were corrected for sample holder and diamagnetic core contributions.

3. RESULTS AND DISCUSSION

The compounds $Na_2Ae_3Sb_4$ for Ae = Ba, Sr are readily obtained by direct reactions, but not the bismuth analogues. Table 2 contains the atomic positional and the isotropic and anisotropic displacement parameters for $Na_2Ba_3Sb_4$, while Table 3 lists the important bond distances therein. All Sb atoms are dimerized as dumbbells Sb_2^{4-}, and these are separated by Ba and Na cations. Figure 1 shows a [100] view of a unit cell of $Na_2Ba_3Sb_4$. The structure consists of three independent layers of atoms perpendicular to the b axis: the first layer around $y = 0$ contains $(Sb3)_2$ dimers (open circles); the second, Ba and M (= 0.5 Ba + 0.5 Na) atoms, black and gray, respectively; the third, Sb1–Sb2 dimers and Na atoms (crossed open circles). As detailed in

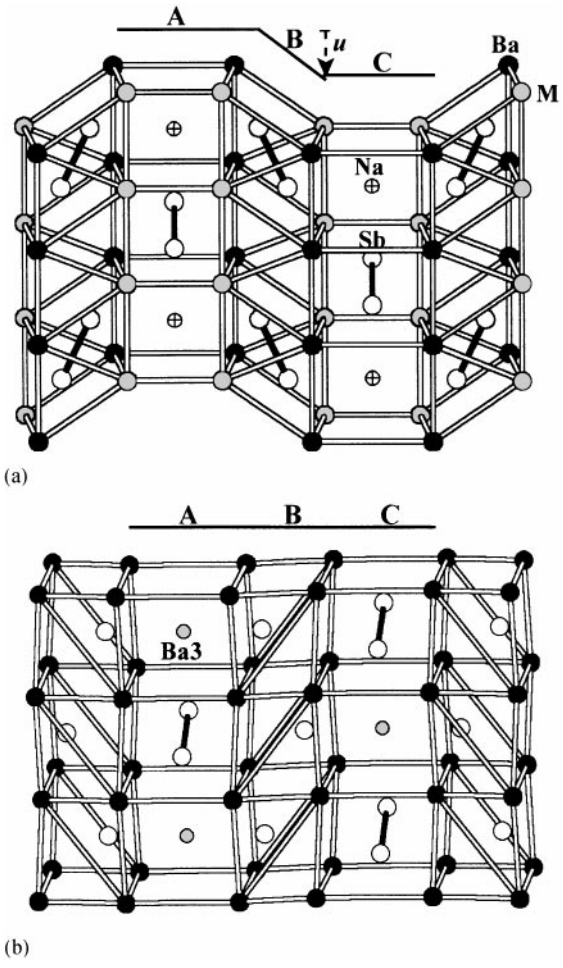

FIG. 3. ~[001] sections of the structures of (a) $Na_2Ba_3Sb_4$ (*Pnma*) and (b) β-Ba_5Sb_4 (*Cmca*, Eu_5As_4), with $\vec{b}$ horizontal in both. Intercation connections shown were selected to illustrate useful polyhedra thereby defined, and do not mark all short separations. The distortion of the more ideal slab B in (b) leads to the Sb3 dimerization in (a) with two fewer electrons.

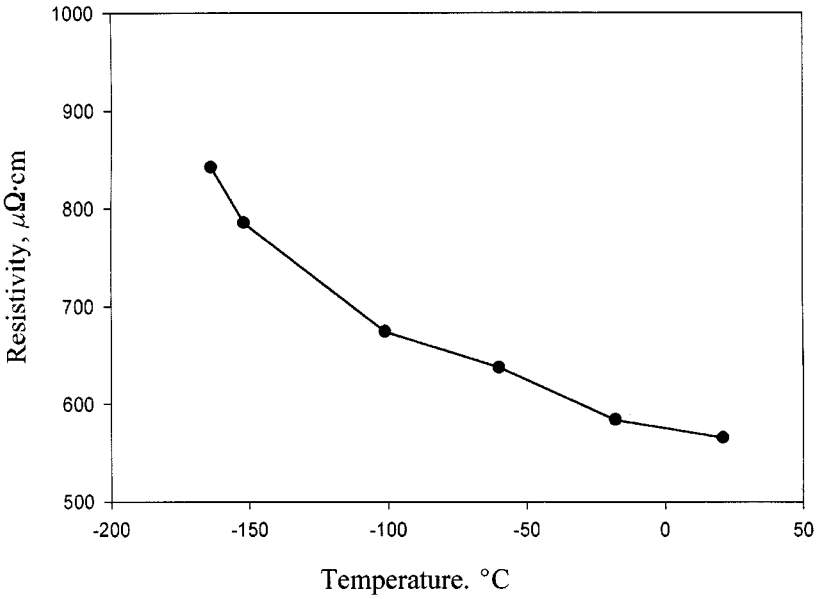

FIG. 4. The resistivities of $Na_2Ba_3Sb_4$ ($\mu\Omega \cdot$cm) by the Q method as a function of temperature (°C).

Fig. 2 (and Table 3), the Sb1–Sb2 dimers are unsymmetrically surrounded by cations, seven around Sb1, namely, two Ba, four *M* and one Na (plus Sb2) (top), and eight around Sb2, viz., four Ba, two *M*, and two Na (plus Sb1) (middle). The larger number of neighbors about Sb2 are 0.06–0.2 Å farther away than for the same cation types around Sb1. Each atom in the Sb3 dimer, which lies on an inversion center, is similarly surrounded by seven close cation neighbors (bottom in the Fig.), three Ba (plus another 0.35 Å more distant that is not shown), three *M*, and one Na (plus Sb3). The Ba and *M* cations about all Sb generally define approximate trigonal prisms that are augmented on two or three side faces by Na and the other Sb; the Sb2 environment is viewed along the pseudo 3-fold axis whereas those axes for Sb1 and Sb3 lie vertical in Fig. 2. The disorder of 50% Na with Ba on only one site (*M*) is reflected by an average distance to Sb that is 0.16 Å (4.7%) less than that around Ba. As far as the bond distances of Sb1–Sb2 = 2.858(2) Å and Sb3–Sb3 = 2.897(2) Å, the latter is close to those in both α- and β-Ba_5Sb_4, 2.885 and 2.886(3) Å, respectively (14, 15). The former Sb1–Sb2 separation may be shorter because the Sb2 atoms have fewer higher field Na and *M* neighbors on the back side. On the other hand, our distance values in the dimers are effectively the same as those found by Eisenmann *et al.* in $K_2Ba_3Sb_4$ (2.856(2), 2.899(2) Å) in which the cations on both Ba (8*d*) sites are disordered (27), but shorter than the 2.923(2) Å found in Cs_4Sb_2 (28). The disorder just noted presumably arises because the cations and their cavities are less differentiated by size.

As before (18), the $Na_2Ba_3Sb_4$ structure and its relationship to (*Cmca*) β-Ba_5Sb_4 can be usefully detailed via two-dimensional slabs defined by polyhedra of Ba and *M* (0.5Ba + 0.5Na) atoms when these are viewed approximately along [001], Fig. 3. As shown for $Na_2Ba_3Sb_4$ in Fig. 3a, the vertical slab labelled A is composed of rhombic prisms of cations that share faces and are centered by alternating Na and (Sb1–Sb2) units. The Na cation and the dimer both lie on mirror planes at $y = \frac{1}{4}, \frac{3}{4}$. Slab B around $y = 0, \frac{1}{2}$ is constructed of alternating $(Sb3)_2^{4-}$-centered rhombic prisms and similar vacant polyhedra ("cubes"). Both can also be viewed in terms of pairs of distorted trigonal prisms that share a common square face, the Sb3 atoms on general positions forming dimers across alternate shared faces of pairs of trigonal prisms. The two slabs A and B are arranged along the *b* axis in such a way that Na- and Sb_2-filled rhombic prisms in slab A are respectively linked to filled and vacant rhombic prisms around $(Sb3)_2$ dimers in slab B. This continues in slab C, which is the same as slab A but displaced by the shear in B.

This distorted version is compared with the more regular structure (*Cmca*) of the metallic β-Ba_5Sb_4 (15) in Fig. 3b, which has Ba3 in place of the centering Na^+ in a 4*c* position. In this instance, the environments defined by Ba1 and Ba2 are closer to distorted cubes. (Some short separations are not drawn so as to emphasize this point.) The differences between (b) and (a) can be understood at least qualitatively. Since the radius of Na and the electrostatic repulsion between Na^+ and Ba^{2+} are both smaller, the distances between Na and Ba, and Na and *M* (formerly Ba3 to Ba2 or Ba1, respectively, in the cubes), are reduced in $Na_2Ba_3Sb_4$, and the idealized "cubes" in slab B in Ba_5Sb_4 once occupied by isolated Sb3 atoms squash to give distorted rhombic

prisms. (Note that the M and Ba now alternate in this construction.) Thus slab C, the repeat of A in Ba_5Sb_4, has now been shifted by the distance u along $\vec{a}$ (marked). Simultaneously, the two isolated Sb atoms distributed between nonadjacent trigonal prisms in Ba_5Sb_4 are now bound in adjoining trigonal prisms and connected into Sb_2^{4-} dumbbells in slab B, the two remaining cavities being left vacant. (This is of course driven by the reduced electron count.) Relative to Ba_5Sb_4, the u displacement in $Na_2Ba_3Sb_4$ corresponds to $0.227a$, more than twice that in $Na_2Eu_3As_4$ (17).

It has become customary to assume in the light of structural evidence alone that phases such as the present $Na_2Ae_3Sb_4$ are Zintl phases, viz., closed-shell, diamagnetic, and semiconducting. However, this has not always proven to be true in our recent studies, especially for anions from earlier groups of p-elements (1,2). We have therefore verified these conditions for $Na_2Ba_3Sb_4$. Its resistivity was measured to be $\sim 5.7 \times 10^2\,\mu\Omega\cdot$cm at 294 K, the change at lower temperatures corresponding to a small negative temperature coefficient, $-.26\%\ K^{-1}$, Fig. 4. The corrected magnetic susceptibilities were found to be substantially constant, $\sim -5.3 \times 10^{-5}$ emu/mol (that is, zero within the accuracy of the diamagnetic corrections), over $100 < T < 300$ K, below which an appreciable increase appeared. The latter was considered to be the result of unknown ferromagnetic impurities. It is noteworthy that the corresponding bismuth phases evidently cannot be obtained. Rather the more remarkable, approximately doubly bonded Bi_2^{2-} has been discovered recently in the metallic compounds A_3Bi_2, $A = $ K, Rb, Cs (29).

ACKNOWLEDGMENTS

The authors are indebted to Jerome Ostenson for measurement of the magnetic susceptibility data.

REFERENCES

1. "Chemistry, Structure and Bonding of Zintl Phases and Ions," (S. Kauzlarich, Ed.). VCH Publishers, New York, 1996.
2. J. D. Corbett, *Angew. Chem., Int. Ed.* **39,** 670 (2000).
3. G. S. Smith, Q. Johnson, and A. G. Tharp, *Acta Crystallogr.* **22,** 269, 940 (1967).
4. J. E. Iglesias and H. Steinfink, *J. Less-Common Met.* **26,** 45 (1972).
5. H. Huang, A. O. Pecharsky, V. K. Pecharsky and K. A. Gschneidner, Jr., private communication, 2001.
6. P. Villars and L. D. Calvert. "Pearson's Handbook of Crystallographic Data for Intermetallic Phases," 2nd Ed. Am. Soc. for Metals Int., Metals Park, OH, 1991.
7. V. K. Pecharsky and K. A. Gschneidner, *J. Alloys Compd.* **260,** 98 (1997).
8. G. H. Rao, *J. Phys.: Condens. Matter* **12,** L93 (2000).
9. W. Choe, V. K. Pecharsky, A. O. Pecharsky, K. A. Gschneidner, Jr., V. G. Young, Jr., and G. J. Miller, *Phys. Rev. Lett.* **84,** 4617 (2000).
10. V. K. Pecharsky and K. A. Gschneidner, Jr., *Phys. Rev. Lett.* **78,** 4494 (1997).
11. V. K. Pecharsky and K. A. Gschneidner, Jr., *Adv. Cryog. Eng.* **43,** 1729 (1998).
12. V. K. Pecharsky and K. A. Gschneidner, Jr., *J. Magn. Magn. Mater.* **200,** 44 (1999).
13. A. M. Guloy and J. D. Corbett, unpublished research.
14. Y. Wang, L. D. Calvert, E. J. Gabe, and J. D. Taylor, *Acta Crystallogr. B* **34,** 1962 (1978).
15. E. Brechtel, G. Cordier, and H. Schäfer, *Z. Naturforsch. B* **36,** 1341 (1981).
16. G. Derrien, L. Monconduit, M. Tillard, and C. Belin, *Acta Crystallogr. C* **55,** 1044 (1999).
17. W. Hönle, J. Lin, M. Hartweg, and H.-G. von Schnering, *J. Solid State Chem.* **97,** 1 (1992).
18. K. Vidyasagar, W. Hönle, and H.-G. von Schnering, *J. Alloys Compd.* **235,** 37 (1996).
19. Z. C. Dong and J. D. Corbett, *J. Am. Chem. Soc.* **115,** 11299 (1993).
20. E. A. Leon-Escamilla, W.-M. Hurng, E. S. Peterson, and J. D. Corbett, *Inorg. Chem.* **36,** 703 (1997).
21. S. Kaskel and J. D. Corbett, *Inorg. Chem.* **39,** 778 (2000).
22. E. A. Leon-Escamilla and J. D. Corbett, *J. Alloys Compd.* **265,** 104 (1998).
23. E. A. Leon-Escamilla and J. D. Corbett, *Inorg. Chem.* **40,** 1226 (2001)
24. TEXSAN for Windows: Crystal Structure Analysis Package; Molecular Structure Corp., The Woodlands, TX, 1997.
25. SHELXTL, Bruker AXS, Inc., Madison, WI, 1997.
26. J.-T. Zhao and J. D. Corbett, *Inorg. Chem.* **34,** 378 (1995).
27. B. Eisenmann, C. Gieck, and U. Röhler, *Z. Anorg. Allg. Chem.* **625,** 1331 (1999).
28. C. Hirschle and C. Röhr, *Z. Anorg. Allg. Chem.* **626,** 1992 (2000).
29. F. Gascoin and S. C. Sevov, *J. Am. Chem. Soc.* **122,** 10251 (2000).